ChemPubSoc Europe

DOI: 10.1002/cmdc.201600122

CHEMMEDCHEM Full Papers

Synthesis, Biochemistry, and Computational Studies of Brominated Thienyl Chalcones: A New Class of Reversible MAO-B Inhibitors

Bijo Mathew[+],*[a] Abitha Haridas,[b] Gülberk Uçar[+],*[c] Ipek Baysal,[c] Monu Joy,[d] Githa E. Mathew,[e] Baskar Lakshmanan,[b] and Venkatesan Jayaprakash[f]

A series of (2*E*)-1-(5-bromothiophen-2-yl)-3-(*para*-substituted phenyl)prop-2-en-1-ones (**TB1**–**TB11**) was synthesized and tested for inhibitory activity toward human monoamine oxidase (hMAO). All compounds were found to be competitive, selective, and reversible toward hMAO-B except (2*E*)-1-(5-bromothiophen-2-yl)-3-(4-nitrophenyl)prop-2-en-1-one (**TB7**) and (2*E*)-1-(5-bromothiophen-2-yl)-3-(4-chlorophenyl)prop-2-en-1-one (**TB8**), which were selective inhibitors of hMAO-A. The most potent compound, (2*E*)-1-(5-bromothiophen-2-yl)-3-[4-(dimethylamino)phenyl]prop-2-en-1-one (**TB5**), showed the best inhibitory activity and higher selectivity toward hMAO-B, with K_i and SI values of 0.11 ± 0.01 μM and 13.18, respectively. PAMPA assays for all compounds were carried out in order to evaluate the capacity of the compounds to cross the blood–brain barrier. Moreover, the most potent MAO-B inhibitor, **TB5**, was found to be nontoxic at 5 and 25 μM, with 95.75 and 84.59% viability among cells, respectively. Molecular docking simulations were carried out to understand the crucial interactions responsible for selectivity and potency.

Introduction

Monoamine oxidase A and B (MAO-A and MAO-B) are the two isoenzymes responsible for catalyzing oxidative deamination of neurotransmitters and dietary amines.[1] Increased MAO-A and B activity is associated with decreased quantities of endogenous and exogenous monoamines.[2] Inhibition of these enzymes has been proposed for the treatment of various pathogeneses in the central nervous system (CNS) precipitated by increased metabolism of biogenic amines.[3] Administration of MAO-A inhibitors results in benefits for the treatment of anxiety and depression.[4] MAO-B inhibitors are frequently used in combination with levodopa (L-Dopa) and may safeguard the depleted supply of dopamine in the Parkinsonian brain and prolong the activity of dopamine derived from its metabolic precursor, L-Dopa.[5,6] This combination therapy allows for the effective L-Dopa dose to be decreased.[7] It should be noted that activity and density of MAO-B in the CNS increase with age, while MAO-A activity remains unchanged. The inhibition of MAO-B-catalyzed oxidation of dopamine is therefore of enhanced relevance in the aged Parkinsonian brain.[8]

Depending on their interactions with MAO isoforms, bound inhibitors are categorized as reversible or irreversible. Many older generations of MAO inhibitors are nonselective in nature but are commonly recognized as antidepressant agents.[9] However, this type of inhibition has been shown to induce significant toxic effects, mainly provoked by inhibition of the peripheral MAOs located in the gut, liver, and endothelium. Irreversible inhibition of intestinal MAO-A permits the production of excessive amounts of tyramine in the systemic circulation, which can induce the release of norepinephrine from peripheral neurons. This state leads to a potentially fatal increase in blood pressure (cheese effect).[10] Currently used hMAO-B inhibitors include selective and irreversible types. These molecules display the typical drawbacks of long-lasting enzyme inhibition, target disruption, poor pharmacokinetic parameters, and potential immunogenicity of enzyme–inhibitor adducts. However, a recently developed and novel class of reversible inhibitors has safer profiles.[11] As the general body of information grows, it is prudent to continue to design new selective and reversible MAO-B inhibitors to be used as various neurodegenerative diseases with higher specificities and fewer deleterious side effects.

[a] *B. Mathew*[+]
Division of Drug Design and Medicinal Chemistry Research Laboratory, Department of Pharmaceutical Chemistry, Ahalia School of Pharmacy, Palakkad 678557, Kerala (India)
E-mail: bijovilaventgu@gmail.com

[b] *A. Haridas, Dr. B. Lakshmanan*
Department of Pharmaceutical Chemistry, Grace College of Pharmacy, Palakkad 678004, Kerala (India)

[c] *Prof. Dr. G. Uçar,[+] I. Baysal*
Department of Biochemistry, Faculty of Pharmacy, Hacettepe University, 06100 Sıhhiye, Ankara (Turkey)
E-mail: gulberk@hacettepe.edu.tr

[d] *M. Joy*
School of Pure & Applied Physics, Mahatma Gandhi University, Kottayam 686560, (India)

[e] *G. E. Mathew*
Department of Pharmacology, Grace College of Pharmacy, Palakkad 678004, Kerala (India)

[f] *Dr. V. Jayaprakash*
Department of Pharmaceutical Sciences and Technology, Birla Institute of Technology, Mesra, Ranchi 835215, Jharkhand (India)

[+] *These authors contributed equally to this work.*

Chalcones (1,3-diaryl-2-propen-1-ones) and their heterocyclic analogues are considered to be open chain flavonoids, which display a number of interesting biological properties. Chalcones may exist in two geometric isomeric forms, *cis* and *trans*, with the *trans* isomer being the most thermodynamically stable.[12–16] As chalcones are relatively easy to prepare, large numbers of derivatives can be synthesized by substituting with various aromatic and heteroaromatic nuclei. In fact, chalcones have been used as promising intermediates in the synthesis of pyrazoline derivatives as part of an effort to discover novel MAO inhibitors.[17,18] The MAO inhibitory activities of chalcones reported by different groups revealed that these compounds show a higher degree of MAO-B inhibition than MAO-A inhibition. Most studies show that the presence of lipophilic electron-withdrawing groups such as chlorine, fluorine, and trifluoromethyl groups at the *para* position on ring B of chalcones increases MAO-B inhibitory activity. These groups may increase the lipophilic character of chalcones, which favors interaction with the entrance cavity of the MAO-B active site.[19–27]

Recently, our research group has reported a number of potent, selective, and reversible inhibitors of hMAO-B, including methoxylated and thiophene-based chalcones with fluoro and trifluoromethyl substitutions. Among these, (2*E*)-1-(4-methoxyphenyl)-3-[4-(trifluoromethyl)phenyl]prop-2-en-1-one and (2*E*)-1-(thiophen-2-yl)-3-[4-(trifluoromethyl)phenyl]prop-2-en-1-one exhibited K_i values of 0.22 ± 0.01 and 0.90 ± 0.05 μM, respectively, toward hMAO-B. The study mainly highlighted the effect of orientation of the fluorine and trifluoromethyl groups on ring B of chalcone on hMAO inhibition.[28,29] Based on the above consideration of the importance of selective and reversible MAO-B inhibitors, this attempt mainly focused on bromo-substituted thienyl chalcones with a variety of electron-donating and -withdrawing groups at the *para* position on phenyl ring B. Information regarding the effect of various groups at the *para* position on ring B of brominated thienyl chalcones and their effect on MAO inhibition has not been explored so far.

Results and Discussion

Chemistry

Brominated thienyl chalcone derivatives (**TB1**–**TB11**) were efficiently synthesized according to the pathway shown in Scheme 1. The chemical structures of the compounds were characterized by means of their ^{1}H NMR, ^{13}C NMR, and mass spectroscopic (MS) data. ^{1}H NMR spectra showed peaks from eight protons comprising signals from the α,β unsaturated unit, the bromine-substituted thiophene, and the mono-substituted phenyl system. It has been noted that the upfield proton of the α-carbon (α-C) and the downfield proton of the β-carbon (β-C) coupled with the methine proton with a coupling constant of 16.0 Hz. This large coupling constant value confirms the presence of *trans* configuration in the brominated thienyl chalcones. Protons belonging to the to the aromatic ring and thiophene ring were observed, with expected chemical shifts and integral values. ^{13}C NMR spectra displayed carbonyl carbons for **TB1**–**TB11** between δ 180.0–181.0. The α-C and β-C of chalcones were assigned as 119.5–121.4 and 144.4–147.0, respectively. Characteristic peaks were observed in the mass spectra of the synthesized compounds. The presence of a bromine atom in all compounds showed characteristic [*M*+2] isotope peaks. All compounds showed satisfactory results by elemental analysis. The structure of **TB5** was solved using single crystal X-ray diffractometry (Figure 1).

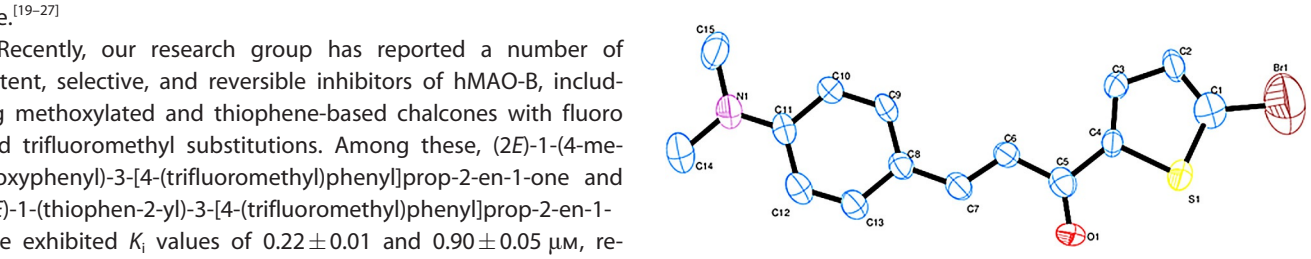

Scheme 1. Synthesis of brominated thienyl chalcones. *Reagents and conditions*: a) C_2H_5OH, 40% KOH, 4 h, room temperature.

Figure 1. ORTEP diagram of lead molecule **TB5**.

Pharmacological evaluation

MAO inhibition studies

Newly synthesized brominated thiophene chalcones were screened for their inhibitory activities toward human MAO isoforms using recombinant enzymes. Enzymatic activities were determined according to a previous method using the Amplex Red MAO assay kit.[40–42] Compounds and reference inhibitors (moclobemide, selegiline, and lazabemide) were independently treated with Amplex Red reagent before the experiment. None of the compounds interfered with the measurements. Test compounds also did not interact with resorufin, as the fluorescence signal did not change when the test and reference compounds were treated with various concentrations of resorufin. Specific enzymatic activities were calculated as 155.12 ± 9.41 pmol mg^{-1} min^{-1} (n = 3) for hMAO-A and 136.90 ± 8.85 pmol mg^{-1} min^{-1} (n = 3) for hMAO-B. The experimental results are shown in Table 1. Selectivity indexes (SI) were expressed as K_i(MAO-A)/K_i(MAO-B). Selectivity toward MAO-A increases as the corresponding SI decreases, while selectivity toward MAO-B increases as the corresponding SI increases.

With the exception of **TB7** and **TB8**, which were selective MAO-A inhibitors, all other derivatives inhibited hMAO-B potently and selectively with a competitive mode of inhibition. Some structure–activity relationships (SARs) were inferred from the data from enzymatic experiments. All synthesized compounds contained a *para*-substituted phenyl moiety attached

Table 1. hMAO inhibitory activities of brominated thiophene-based chalcones.

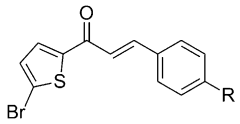

Compound	R	K_i [μM][a] MAO-A	K_i [μM][a] MAO-B	SI[b]	Inhibition type	Reversibility	MAO selectivity
TB1	H	4.55 ± 0.27	1.22 ± 0.10	3.73	competitive	reversible	MAO-B
TB2	OH	2.85 ± 0.11	1.02 ± 0.09	2.79	competitive	reversible	MAO-B
TB3	OCH_3	1.40 ± 0.10	0.55 ± 0.11	2.54	competitive	reversible	MAO-B
TB4	CH_3	2.54 ± 0.17	0.31 ± 0.01	8.20	competitive	reversible	MAO-B
TB5	$N(CH_3)_2$	1.45 ± 0.09	0.11 ± 0.01	13.18	competitive	reversible	MAO-B
TB6	CH_2CH_3	1.25 ± 0.09	0.19 ± 0.01	6.57	competitive	reversible	MAO-B
TB7	NO_2	0.54 ± 0.03	3.05 ± 0.15	0.18	competitive	reversible	MAO-A
TB8	Cl	0.50 ± 0.03	9.30 ± 0.62	0.05	competitive	reversible	MAO-A
TB9	Br	1.05 ± 0.09	0.25 ± 0.01	4.20	competitive	reversible	MAO-B
TB10	F	4.06 ± 0.19	1.71 ± 0.12	2.37	competitive	reversible	MAO-B
TB11	CF_3	3.85 ± 0.20	0.96 ± 0.07	4.01	competitive	reversible	MAO-B
moclobemide	–	0.15 ± 0.01	1.75 ± 0.14	0.09	competitive	reversible	MAO-A
selegiline	–	6.55 ± 0.40	0.14 ± 0.01	46.79	suicide	irreversible	MAO-B
lazabemide	–	547.22 ± 21.30	0.007 ± 0.001	78.17	competitive	reversible	MAO-B

[a] Values are the mean ± SEM of three independent experiments. [b] Selectivity index, calculated as K_i(MAO-A)/K_i(MAO-B); selectivity toward MAO-A increases as the corresponding SI decreases, while selectivity toward MAO-B increases as the corresponding SI increases.

to the 5-bromo thiophene by an enone linker. Among the synthesized derivatives, nine compounds showed good inhibition of MAO-B in the sub-micromolar range. The most potent compound, **TB5**, with a dimethylamino group at the *para* position of the phenyl system showed the best activity and higher selectivity toward hMAO-B, with K_i and SI values of 0.11 ± 0.01 μM and 13.18, respectively. Its inhibitory potency was found to be higher than that of selegiline but less than that of lazabemide. According to the selectivity index, compound **TB5** also appeared to be the most selective hMAO-B inhibitor in this series. However, the selectivity of **TB5** toward hMAO-B was less than that of lazabemide and selegiline (SI values for selegiline and lazabemide were calculated as 46.79 and 78.17, respectively). Among the synthesized brominated thienyl chalcones, the presence of electron-donating groups such as dimethylamino, ethyl, methyl, and methoxy groups at the *para* position on the phenyl ring were found to be selective toward MAO-B. The presence of a halogen, such as a chlorine or bromine atom, on the phenyl ring showed mixed results for MAO inhibition. Introduction of bromine at the *para* position on the phenyl ring was more beneficial than a fluorine atom for MAO-B inhibition. Chlorine substitution on the phenyl ring showed potent and selective inhibition toward MAO-A, with a K_i value of 0.50 ± 0.03 μM (**TB8**). The following order of MAO inhibitory activity was observed for the brominated thienyl chalcones:

hMAO-A: 4-Cl > 4-NO_2 > 4-Br > 4-C_2H_5 > 4-OCH_3 > 4-*N*-$(CH_3)_2$ > 4-CH_3 > 4OH > 4-CF_3 > 4-F > 4-H

hMAO-B: 4-*N*-$(CH_3)_2$ > 4-C_2H_5 > 4-Br > 4-CH_3 > 4-OCH_3 > 4-CF_3 > 4-OH > 4-H > 4-F > 4-NO_2 > 4-Cl

As a MAO-B inhibitor, compound **TB5** was 11-fold more potent than parent compound **TB1**. This clearly suggests that the enhanced anti-MAO-B activity of **TB5** is due to the presence of a lipophilic electron-donating dimethyl group on the phenyl system. Introduction of an electron-withdrawing group, such as a chlorine or nitro group, on the phenyl system dramatically abated anti-MAO-B activity and selectivity but improved the anti-MAO-A activity. Using the high inhibition potency and MAO-B selectivity from enzymatic studies as selection criteria, **TB5** was considered a promising lead compound for the development and optimization of selective MAO-B inhibitors for various neurodegenerative diseases.

Kinetics studies

Kinetic analyses were carried out for the most potent MAO-B inhibitor (**TB5**) and MAO-A inhibitor (**TB8**) from this series to gain further insight into the mode of MAO inhibition. A set of Lineweaver–Burk plots were constructed in the absence and presence of various concentrations of compounds **TB5** and **TC8**. The set consisted of five graphs, each constructed by measuring MAO-B and MAO-A catalytic rates at different substrate concentrations (0.1–1 μM). The first Lineweaver–Burk plot was constructed in the absence of inhibitor, while the remaining four graphs were constructed in the presence of different concentrations of **TB5** and **TB8**. The observation that the lines were linear and intersected the y-axis suggested that **TB5** and **TB8** interacts with the catalytic site of hMAO-B and hMAO-A with a competitive mode of inhibition (Figures 2 and 3). Replots of the slopes of the Lineweaver–Burk plots versus inhibitor concentrations are shown in Figures 4 and 5, and the K_i values were estimated as 0.11 and 0.50 μM for **TC5** (hMAO-B) and **TB8** (hMAO-A), respectively.

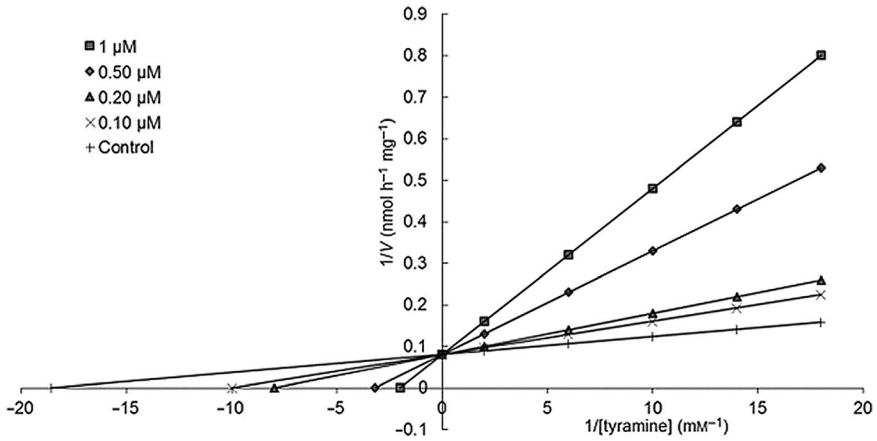

Figure 2. Lineweaver–Burk plots of hMAO-B activity in the absence and presence of various concentrations of compound **TB5**.

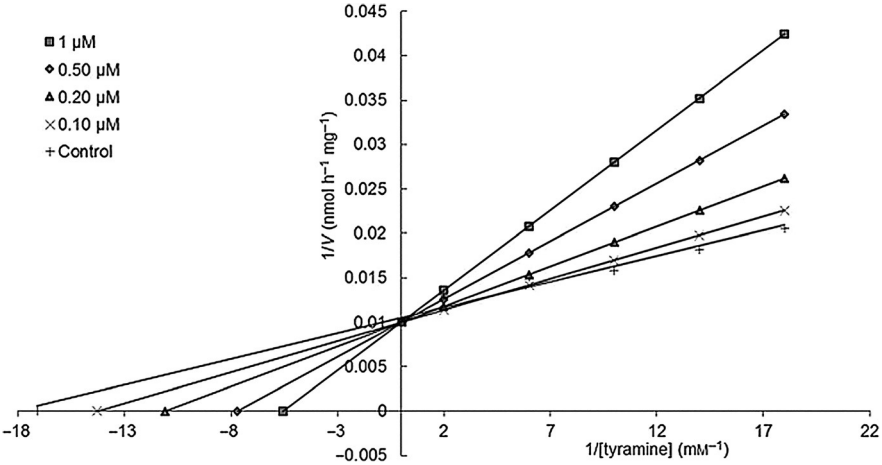

Figure 3. Lineweaver–Burk plots of hMAO-A activity in the absence and presence of various concentrations of compound **TB8**.

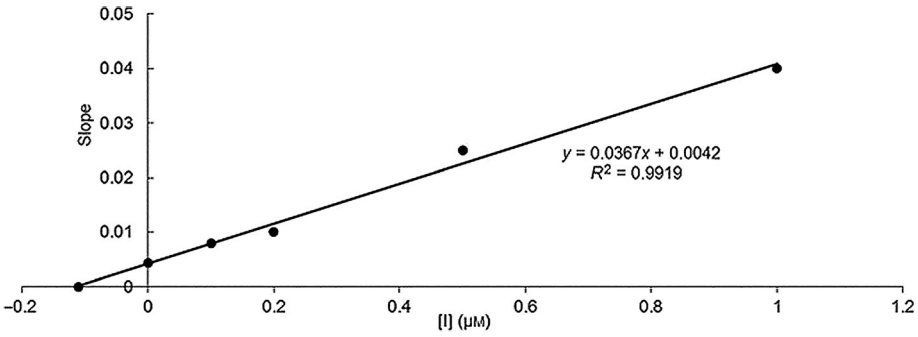

Figure 4. Replots of the slopes of the Lineweaver–Burk plots versus inhibitor **TB5** concentration (hMAO-B).

Reversibility studies

Competitive reversible inhibitors have less influence in the MAO enzyme recovery after withdrawal, as the ingested tyramine is able to displace the inhibitor from the MAO active site and is metabolized in the normal way by the peripheral enzyme in the gut and liver. Moreover, reversible MAO-B inhibitors have significant advantages over irreversible inhibitors for the management of Parkinson's disease.[30] All tested compounds in the present study inhibited the hMAO isoforms reversibly. Table 2 presents the reversibility of hMAO-B inhibition for the novel compounds. The reversibility of MAO inhibition by brominated thiophene chalcones was investigated by determination of the recovery of MAO activity after dialysis of enzyme–inhibitor mixtures. MAO isoforms were incubated in the presence of the inhibitors at concentrations fivefold higher

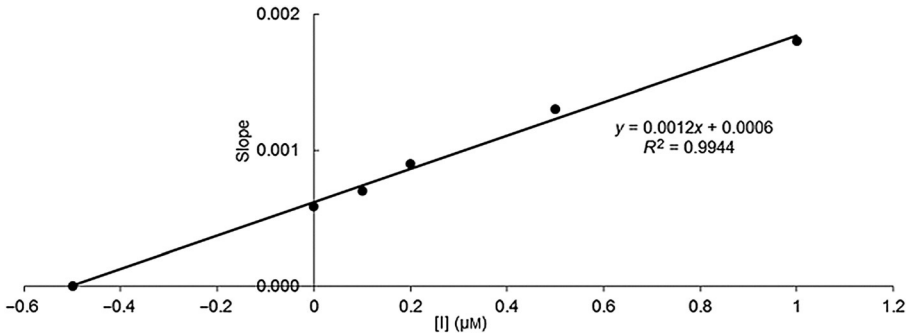

Figure 5. Replots of the slopes of the Lineweaver–Burk plots versus inhibitor **TB8** concentration (hMAO-A).

Table 2. Reversibility of hMAO activity by brominated thienyl chalcones.

Compound	hMAO-A activity [%][a] before washing	hMAO-A activity [%][a] after washing	hMAO-B activity [%][a] before washing	hMAO-B activity [%][a] after washing	Reversibility
no inhibitor	100 ± 0.00	100 ± 0.00	100 ± 0.00	100 ± 0.00	–
moclobemide	38.02 ± 2.00	88.00 ± 4.96	99.50 ± 5.22	95.01 ± 4.55	reversible
selegiline	90.16 ± 4.82	88.33 ± 4.30	50.99 ± 2.05	53.44 ± 2.75	irreversible
lazabemide	98.00 ± 3.90	99.00 ± 4.05	20.55 ± 1.96	88.22 ± 4.09	reversible
TB1	80.22 ± 4.96	89.87 ± 3.00	59.00 ± 2.26	94.22 ± 5.00	reversible
TB2	77.60 ± 3.46	89.29 ± 5.74	58.25 ± 2.19	95.00 ± 5.36	reversible
TB3	79.90 ± 3.11	88.25 ± 3.96	61.22 ± 3.45	86.27 ± 4.00	reversible
TB4	80.33 ± 4.12	90.01 ± 4.60	48.00 ± 2.66	89.90 ± 4.77	reversible
TB5	97.31 ± 3.80	88.26 ± 5.31	37.23 ± 1.74	97.57 ± 4.61	reversible
TB6	81.22 ± 3.60	91.99 ± 4.11	57.00 ± 2.05	96.25 ± 2.00	reversible
TB7	67.20 ± 2.90	87.90 ± 4.00	81.29 ± 3.64	95.00 ± 3.87	reversible
TB8	40.22 ± 2.47	97.85 ± 4.00	87.25 ± 2.90	93.55 ± 4.22	reversible
TB9	80.22 ± 4.13	91.00 ± 4.68	54.33 ± 2.90	92.66 ± 4.10	reversible
TB10	81.96 ± 4.21	92.00 ± 3.77	69.16 ± 3.22	93.56 ± 4.32	reversible
TB11	85.63 ± 3.75	97.22 ± 230	66.55 ± 3.54	94.10 ± 4.36	reversible

[a] Values are the mean ± SEM of three independent experiments.

than the IC_{50} values for a period of 15 min and subsequently dialyzed for 24 h. hMAO-B inhibition by compound **TB5** and hMAO-A inhibition by compound **TB8** were completely reversed after 24 h of dialysis.

Results suggested that brominated thienyl chalcones are reversible inhibitors of hMAO isoforms and have considerable advantages over irreversible inhibitors, which may possess serious pharmacological side effects. The potent and selective MAO-B inhibitor selegiline has been reported to have severe side effects due to its amphetamine metabolites, and both selegiline and rasagiline are irreversible MAO-B inhibitors, triggering pharmacological side effects in long-term treatment of Parkinson's disease.[31,32] Compound **TB5** exhibited good reversibility of hMAO-B inhibition in the present series. The reversibility values for compound **TB5** was calculated as 37.23 ± 1.74 and 97.57 ± 4.61 before and after dialysis, respectively.

In vitro blood–brain barrier (BBB) permeation assay

The blood–brain barrier (BBB) has great value for the delivery of drugs to the CNS. The BBB consists of several barriers in parallel, with the two best-described barriers being the vascular BBB, consisting primarily of the capillary bed, and the blood–cerebrospinal fluid (blood–CSF) barrier, consisting primarily of the choroid plexus.[33] The BBB is nonselective toward drug uptake by diffusion or active transport and creates major hurdles for successful CNS drug development. Molecules like glucose and fat-/lipid-soluble drugs can rapidly cross into the brain, while delivery of many drugs into the brain is difficult because of their poorly fat-soluble nature.[34]

To evaluate the potential for the newly synthesized chalcone derivatives to cross the BBB, a parallel artificial membrane permeation assay (PAMPA) for the BBB was performed. Assay validation was performed by comparing experimental permeabilities of nine commercial drugs with reported values (Table 3). A plot of experimental data versus literature values gave a good linear correlation of $R^2 = 0.9934$ (Figure 6). According to the limits established by Di et al. for BBB permeation, test compounds were classified as follows:[35]

CNS+ (high predicted BBB permeation): P_e (10^{-6} cm s^{-1}) > 4.00

CNS− (low predicted BBB permeation): P_e (10^{-6} cm s^{-1}) < 2.00

CNS± (uncertain BBB permeation): P_e (10^{-6} cm s^{-1}) from 4.00 to 2.00.

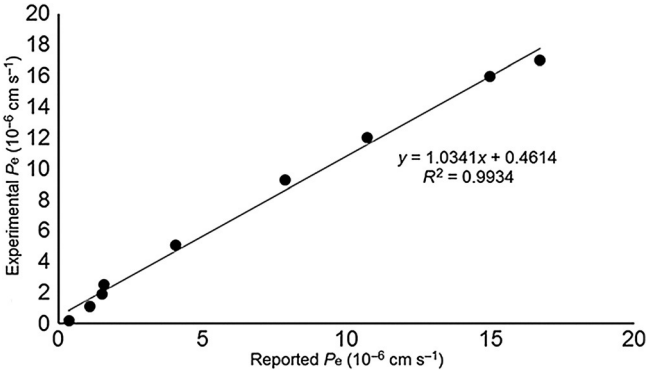

Figure 6. Linear correlation between experimental and reported permeability of commercial drugs using the PAMPA BBB assay.

Table 3. Experimental permeability in the PAMPA BBB assay of brominated thiophene chalcones and commercial drugs used for assay validation.

Compound[a]	Literature[b] P_e [10^{-6} cm s^{-1}][c]	Experimental P_e [10^{-6} cm s^{-1}][c]	Prediction
testosterone	17.0	16.72 ± 1.52	CNS +
verapamil	16.0	14.97 ± 1.65	CNS +
β-estradiol	12.0	10.72 ± 1.69	CNS +
progesterone	9.3	7.88 ± 0.33	CNS +
corticosterone	5.1	4.08 ± 1.03	CNS +
piroxicam	2.5	2.23 ± 0.53	CNS ±
hydrocortisone	1.8	1.53 ± 0.48	CNS −
lomefloxacin	1.1	1.09 ± 0.23	CNS −
dopamine	0.2	0.36 ± 0.14	CNS −
TB1	–	6.45 ± 0.96	CNS +
TB2	–	6.67 ± 2.06	CNS +
TB3	–	8.41 ± 2.25	CNS +
TB4	–	8.22 ± 1.79	CNS +
TB5	–	15.08 ± 1.60	CNS +
TB6	–	9.72 ± 1.58	CNS +
TB7	–	5.72 ± 1.23	CNS +
TB8	–	10.25 ± 1.67	CNS +
TB9	–	9.96 ± 2.68	CNS +
TB10	–	8.02 ± 1.02	CNS +
TB11	–	5.19 ± 0.92	CNS +

[a] Compounds were dissolved in DMSO (5 mg mL^{-1}) and diluted with PBS/EtOH (70:30); final compound concentration: 100 μg mL^{-1}. [b] Taken from ref. [35]. [c] Values are expressed as the mean ± SD of three independent experiments; –: no published details available.

The data listed in Table 3 indicated that all of the brominated thiophene chalcones could cross the BBB to target the enzyme in the CNS. Compounds **TB5**, **TB8**, **TB9**, and **TB6** showed the highest permeability, suggesting that they may be able to cross the BBB and reach biological targets located in the CNS, consistent with our design strategy. These results also encouraged us to carry out more detailed studies with these new prodrugs.

Cytotoxicity studies

In vitro cytotoxicity of brominated thiophene chalcones and standard MAO inhibitors were tested in human HepG2 hepatic cancer cells at three different concentrations (1–25 μM) (Table 4). The results showed that most of the novel compounds were not toxic to hepatic cells at 1 μM concentration. At 5 μM, compounds **TB5**, **TB7**, **TB8**, **TB9**, and **TB10** were completely nontoxic to the cells. The most potent MAO-B inhibitor of the present series, **TB5**, was nontoxic at 5 and 25 μM, resulting in cell viabilities of 95.75% and 84.59%, respectively. It was noted that the presence of a nitrogen substituent, like a dimethylamino or nitro group, was responsible for the lower degrees of cytotoxicity of **TB5** and **TB7** at 25 μM, with 84.59% and 76.81% cell viability, respectively. The presence of a dibromo atom, both on thiophene and the phenyl ring of compound **TB9** showed the lowest cytotoxicity at 25 μM, with 92.86% cell viability in this series. Interestingly, the toxicity for unsubstituted compound **TB1** was greater than that of other substituted heteroaryl chalcones at 25 μM in HepG2 cells.

Table 4. In vitro cytotoxicity of brominated thiophene chalcones in HepG2 cells.

Compound	Viability [%] 1 μM	5 μM	25 μM
moclobemide	95.70 ± 4.26	77.22 ± 2.90[a]	56.20 ± 2.34[b]
selegiline	95.88 ± 2.05	89.78 ± 2.60[a]	60.05 ± 2.05[b]
lazabemide	96.00 ± 3.85	90.25 ± 4.12[a]	58.00 ± 2.91[b]
TB1	97.21 ± 3.05	92.00 ± 4.12[a]	42.69 ± 1.18[c]
TB2	84.51 ± 2.75[a]	60.70 ± 2.16[b]	50.16 ± 2.45[b]
TB3	85.62 ± 0.87[a]	60.86 ± 2.07[b]	57.67 ± 2.18[b]
TB4	96.01 ± 2.31	75.79 ± 2.23[b]	66.99 ± 1.53[b]
TB5	97.50 ± 2.02	95.75 ± 3.56	84.59 ± 2.54[a]
TB6	94.21 ± 2.59	70.97 ± 2.11[b]	55.83 ± 2.21[b]
TB7	96.34 ± 4.10	91.17 ± 2.24	76.81 ± 1.59[b]
TB8	97.00 ± 1.45	94.82 ± 2.21	44.43 ± 2.24[b]
TB9	95.54 ± 3.36	93.29 ± 1.64	92.86 ± 1.49[a]
TB10	97.67 ± 1.45	93.46 ± 3.55	59.98 ± 1.17[b]
TB11	98.01 ± 1.53	92.43 ± 1.44[a]	83.30 ± 1.65[a]

Data are the mean ± SEM of $n = 3$ experiments. Cell viability is expressed as a percentage of the control value; $p < 0.05$ was considered statistically significant ([a] $p < 0.05$; [b] $p < 0.01$; [c] $p < 0.001$ vs. control).

Molecular docking studies

Binding interaction analysis of MAO-B inhibitor TB5

To carry out a detailed study of the hypothetical MAO-B binding modes of the brominated thienyl chalcones, molecular docking studies were performed. The active site of MAO-B is characterized by two large pockets. Pocket 1 involves a large aromatic cage made up of FAD, Phe 343, and four tyrosine residues: Tyr 188, 189, 435, and 398. Pocket 2 is a hydrophobic pocket characterized by Leu 171, Tyr 326, Phe 168, Ile 198, and Ile 199. The smaller entrance cavity with Ile 199 effectively serves as a gate between these cavities.[36] Depending on the structural nature of the bound inhibitor, the two cavities may be either separate or fused.[37]

The docking poses of MAO-B inhibitors suggest that the terminal lipophilic groups such as dimethylamino, ethyl, bromo, methyl, and methoxy at the *para* position on the chalcone phenyl rings project into the entrance cavity of MAO-B, where van der Waals interactions are predominant. The presence of a bulky lipophilic dimethylamino group at the *para* position on ring B of brominated thienyl chalcone **TB5** can efficiently navigate Ile 199 and span both entrance and substrate cavities. Docking studies of lead compound **TB5** led to the proposed binding mode in which a 5-bromo-substituted thiophene binds pocket 1 and is anchored in the substrate cavity close to the FAD cofactor, with a lipophilic dimethylamino positioned in the entrance cavity of MAO-B. The interaction is stabilized by the strong π–π stacking interaction between the phenyl system of the chalcone and the FAD unit (Figure 7). The rotatable bonds present in the compound result in a non-coplanar confirmation between the phenyl system and the halogenated thiophene and can make tight interactions in the inhibitor binding cavity of MAO-B without any hydrogen bonding interactions. These data provide evidence that MAO-B inhibitory potency results from having a structure that binds to both the entrance and substrate cavities.

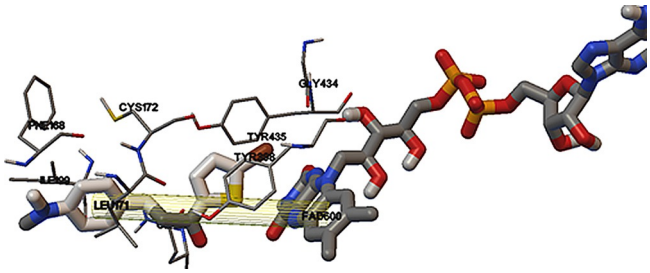

Figure 7. Docking pose of **TB5** in the MAO-B active site. Yellow mesh indicates π–π stacking interaction.

Binding interaction analysis of MAO-A inhibitor TB8

The inhibitor binding site of MAO-A is a single cavity that extends from the flavin ring to the cavity-shaping loop.[38] **TB8** oriented the active site of MAO-A in such a way that the α,β-unsaturated carbonyl linker oriented toward pocket 1 of the aromatic cage lined by (FAD, Tyr 407, and Tyr 444). This places the 5-bromo-substituted thiophene ring in pocket 2 (defined by Ile 180, Ile 335, Leu 337, and Phe 352) and the *para*-chloro phenyl ring in pocket 3 (defined by Gly 74, Ile 207, Phe 208, Glu 216, and Trp 441). **TB8** is mainly stabilized by the phenyl B ring and bromo-substituted thiophene A ring, making a strong π–π stacking interaction with Phe 352 in pocket 2 of MAO-B (Figure 8). This stabilizing interaction results in the enone linker of thienyl chalcone being within good proximity (2.922 Å) of the isoalloxazine of the FAD unit. This shorter distance between the electron-rich carbonyl oxygen of chalcone and the electron-deficient sp^2 N5 atom of FAD supports its enhanced binding affinities to the inhibitor binding cavity of MAO-A. This allows the formation of a charge-transfer bonding interaction between the drug and the FAD unit, which may be particularly important for MAO-A inhibition.[39]

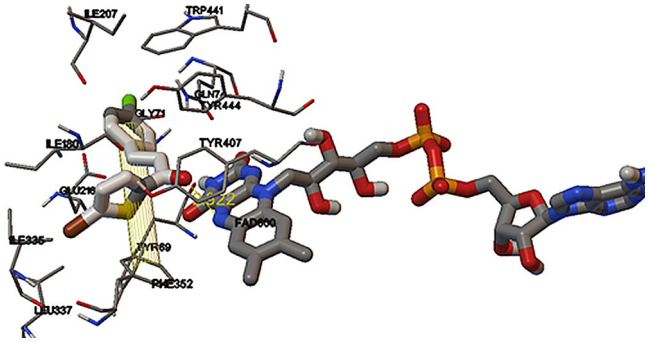

Figure 8. Docking pose of **TB8** in the MAO-A active site. Yellow mesh indicates π-π stacking interaction.

Conclusions

In the present study, a series of brominated thienyl chalcones (**TB1**–**TB11**) were synthesized and evaluated as inhibitors of MAO-A and MAO-B, and inhibitory activity was strongly affected by the type, electron density, and bulkiness of the substituents present at the *para* position on the phenyl ring. This study documented that substitution at the *para* position on the phenyl ring with electron-donating groups yields structures with potent MAO-B inhibitory activities. This behavior was exemplified by **TB5** (K_i = 0.11 μM), **TB6** (K_i = 0.19 μM), **TB4** (K_i = 0.31 μM), and **TB3** (K_i = 0.55 μM), which possess dimethylamino, ethyl, methyl, and methoxy groups, respectively, at the *para* position of phenyl ring. PAMPA assays of all compounds experimentally corroborated the results from MAO inhibition studies. Previously, we reported fluorochalcones from 2-acetyl thiophene, observing that the position of fluorine and trifluoromethyl groups (*ortho*, *meta*, *para*) on ring B had a negligible impact on inhibition of both hMAO-A and hMAO-B. The most potent hMAO-B inhibitor in this series, compound (*2E*)-1-(thiophen-2-yl)-3-[4-(trifluoromethyl)phenyl]prop-2-en-1-one, inhibited the hMAO-B isoform potently and selectively, with a *Ki* value of 0.90 ± 0.05 μM. This compound has a trifluoromethyl substituent at the *para* position of the B ring and is eightfold less potent than **TB5**. From the above observation, we learned that a change in hMAO-B inhibitory activity is due to the nature and position of groups on phenyl ring B and is also greatly influenced by the nature and position of substituents on thiophene ring A. The SAR comparison is outlined in Figure 9.

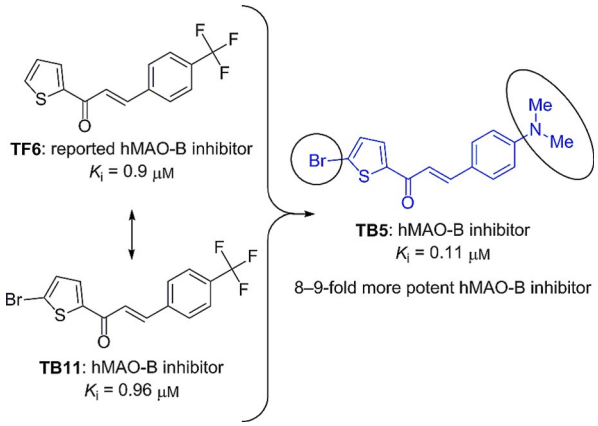

Figure 9. SAR of thienyl chalcones for hMAO-B inhibition.

According to its significantly high hMAO-A inhibitory potency and selectivity, as well as its low toxicity, compound **TB8** appears to be a promising candidate for the management of major depression. Additionally, the reversibility of this compound's inhibitory activity appears to be an advantage for the design and development of new antidepressants. The in vitro BBB prediction of lead MAO-B inhibitor **TB5** showed excellent results and encouraged us to further explore the potential of this family of derivatives as potential lead candidates for the treatment of Parkinson's disease. Recent studies suggest that reversible MAO-B inhibitors might also be effective in treatment of Alzheimer's disease by selective inhibition of astrocytic gamma-aminobutyric acid production, as well as in Parkinson's disease. The development of selective reversible MAO-B inhibitors may reduce the adverse effects of irreversible inhibitors and may be promising compounds for the treatment of other

neurodegenerative diseases. Compound **TB5** may have value as a promising potent and reversible MAO-B inhibitor in this regard. The systematic and finely tuned exploration of the various electron-donating and -withdrawing groups at the *para* position on the phenyl ring of the brominated thienyl chalcone enabled precise development of a new MAO-B inhibitor. Overall, the study provided meaningful information for further development of multifunctional drugs for neurodegenerative disorders such as Parkinson's and Alzheimer's diseases.

Experimental Section

General: 2-Acetyl 5-bromo-thiophene and all substituted benzaldehydes were procured from Sigma–Aldrich USA. Melting points of all synthesized derivatives were determined by the open capillary tube method, and values were uncorrected. ^{1}H NMR and ^{13}C NMR spectra were recorded on a Bruker Avance III 600 spectrometer at frequencies of 400 MHz and 100 MHz, respectively (Bruker, Karlsruhe, Germany). All NMR measurements were conducted in $CDCl_3$, and chemical shifts are reported in parts per million (δ) downfield from the signal of tetramethylsilane added to the deuterated solvent. Mass spectra were recorded on a JEOL GCmate mass spectrometer. Elemental analyses (C, H, N) were performed on a Leco CHNS 932 analyzer.

Synthesis: A mixture of 2-acetyl 5-bromo thiophene (0.01 mol), *para*-substituted benzaldehyde (0.01 mol), and 40% aqueous KOH was added to EtOH (30 mL) and was stirred at room temperature for 2–6 h. The resulting product was stored overnight in the refrigerator. The solid precipitate was filtered, washed with water, and recrystallized from EtOH/acetone/chloroform (1:1:1) to yield pure crystals.

(2*E*)-1-(5-Bromothiophen-2-yl)-3-phenyl prop-2-en-1-one (**TB1**): Compound **TB1** was isolated as an off-white solid (yield: 94%): mp: 106–108 °C; ^{1}H NMR (400 MHz, $CDCl_3$): δ = 6.77–6.73 (d, 1H, J = 16.0 Hz, CH_α), 7.00–6.99 (d, 1H, J = 4.0 Hz, H_4'), 7.14–7.12 (t, 1H, J = 8.0 Hz, H_4), 7.20-.7.18 (d, 2H, J = 8.0 Hz, H_3 and H_5), 7.24–7.22 (d, 2H, J = 8.0 Hz, H_2&H_6), 7.43–7.42 (d, 1H, J = 4.0 Hz, H_3'), 7.63–7.59 ppm (d, 1H, J = 16.0 Hz, CH_β); ^{13}C NMR (100 MHz, $CDCl_3$): δ = 180.1 (C=O), 146.9 (C_2'), 145.4 (C_β), 138.7 (C_3'), 135.2 (C_1), 132.2 (C_4'), 128.5 (C_3 and C_5), 128.1 (C_4), 126.2 (C_2 and C_6), 122.1 (C_5'), 121.1 ppm (Cα); ESI-MS (*m/z*): calculated 248.72, observed 249.16 $[M]^+$, $[M+2]$; Anal. calcd for $C_{13}H_9BrOS$: C 53.26, H 3.09, S 10.89, found: C 53.18, H 3.14, S 10.96.

(2*E*)-1-(5-Bromothiophen-2-yl)-3-(4-hydroxyphenyl)prop-2-en-1-one (**TB2**): Compound **TB2** was isolated as an off-white solid (yield: 96%): mp: 80–82 °C; ^{1}H NMR (400 MHz, $CDCl_3$): δ = 5.28 (s, 1H, OH), 6. 54–6.50 (d, 1H, J = 16.0 Hz, CH_α), 6.67–6.65 (d, 2H, J = 8.0 Hz, H_3 and H_5), 6.89–6.88 (d, 1H, J = 4.0 Hz, H_4'), 7.13–7.11 (d, 2H, J = 8.0 Hz, H_2 and H_6), 7.32–7.31 (d, 1H, J = 4.0 Hz, H_3'), 7.54–7.50 ppm (d, 1H, J = 16 Hz, CH_β); ^{13}C NMR (100 MHz, $CDCl_3$): δ = 181.0 (C=O), 159.3 (C_4), 147.2 (C_2'), 145.9 (C_β), 138.2 (C_3'), 132.3 (C_4'), 128.1 (C_1), 127.4 (C_2 and C_6), 122.3 (C_5'), 121.3 (Cα), 115.8 ppm (C_3 and C_5); ESI-MS (*m/z*): calculated 309.37, observed 310.01 $[M]^+$, $[M+2]$; Anal. calcd for $C_{13}H_9BrO_2S$: C 50.50, H 2.93, S 10.37, found: C 50.87, H 2.82, S 10.25.

(2*E*)-1-(5-Bromothiophen-2-yl)-3-(4-methoxyphenyl)prop-2-en-1-one (**TB3**): Compound **TB3** was isolated as an off-white powder (yield: 68%): mp: 130–132 °C; ^{1}H NMR (400 MHz, $CDCl_3$): δ = 3.86 (s, 3H, OCH_3), 6.95–6.93 (d, 2H, J = 8.0 Hz, H_3 and H_5), 7.14–7.13 (d, 1H, J = 4.0 Hz, H_4'), 7.21–7.17 (d, 1H, J = 16.0 Hz, CH_α), 7.58–7.57 (d, 1H, J = 4.0 Hz, H_3'), 7.60–7.58 (d, 2H, J = 8.0 Hz, H_2 and H_6), 7.83–7.79 ppm (d, 1H, J = 16.0 Hz, CH_β); ^{13}C NMR (100 MHz, $CDCl_3$): δ = 181.0 (C=O), 161.9 (C_4), 147.3 (C_2'), 144.4 (C_β), 131.4 (C_3'), 131.2 (C_4'), 130.3 (C_2 and C_6), 127.3 (C_1), 122.3 (Cα), 118.2 (C_5'), 114.5 (C_3 and C_5), 55.4 ppm (O-CH_3); ESI-MS (*m/z*): calculated 323.20, observed 323.83 $[M]^+$, $[M+2]$; Anal. calcd for $C_{14}H_{11}BrO_2S$: C 52.03, H 3.43, S 9.92, found: C 52.17, H 3.42, S 10.01.

(2*E*)-1-(5-Bromothiophen-2-yl)-3-(4-methylphenyl)prop-2-en-1-one (**TB4**): Compound **TB4** was isolated as an off-white powder (yield: 86%): mp: 108–110 °C; ^{1}H NMR (400 MHz, $CDCl_3$): δ = 2.39 (s, 3H, CH_3), 7.14–7.13 (d, 1H, J = 4.0 Hz, H_3'), 7.23–7.21 (d, 2H, J = 8.0 Hz, H_2 and H_6), 7.29–7.25 (d, 1H, J = 16.0 Hz, CH_α), 7.53–7.51 (d, 2H, J = 8.0 Hz, H_3 and H_5), 7.59–7.58 (d, 1H, J = 4.0 Hz, H_4'), 7.84–7.80 ppm (d, 1H, J = 16.0 Hz, CH_β); ^{13}C NMR (100 MHz, $CDCl_3$): δ = 180.9 (C=O), 147.2 (C_2'), 144.7 (C_β), 141.4 (C_3'), 131.8 (C_4), 131.8 (C_4'), 131.6 (C_3 and C_5), 129.7 (C_2 and C_6), 128.5 (C_1), 122.5 (C_5'), 119.5 (Cα), 21.5 ppm (CH_3); ESI-MS (*m/z*): calculated 307.20, observed 307.79 $[M]^+$, $[M+2]$; Anal. calcd for $C_{14}H_{11}BrOS$: C 54.74, H 3.61, S 10.44, found: C 54.70, H 3.74, S 10.23.

(2*E*)-1-(5-Bromothiophen-2-yl)-3-[4-(dimethylamino) phenyl]-prop-2-en-1-one (**TB5**): Compound **TB5** was isolated as an orange powder (yield: 96%): mp: 132–134 °C; ^{1}H NMR (400 MHz, $CDCl_3$): δ = 3.04 (s, 6H, $N(CH_3)_2$), 6.68–6.66 (d, 2H, J = 8.0 Hz, H_3 and H_5), 7.10–7.08 (d, 2H, J = 8.0 Hz, H_2 and H_6), 7.47–7.46 (d, 1H, J = 4.0 Hz, H_3'), 7.55–7.51 (d, 1H, J = 16.0 Hz, CH_α), 7.55–7.54 (d, 1H, J = 4.0 Hz, H_4'), 7.82–7.78 ppm (d, 1H, J = 16.0 Hz, CH_β); ^{13}C NMR (100 MHz, $CDCl_3$): δ = 180.9 (C=O), 152.2 (C_4), 147.9 (C_2'), 145.8 (C_β), 131.2 (C_3'), 130.7 (C_2 and C_6), 127.8 (C_4'), 122.78 (C_1), 121.4 (Cα), 115.1 (C_5'), 111.8 (C_3&C_5), 40.0 ppm (*N*-(CH_3)$_2$); ESI-MS (*m/z*): calculated 336.24, observed 336.89 $[M]^+$, $[M+2]$; Anal. calcd for $C_{15}H_{14}BrNOS$: C 53.58, H 4.20, S 9.54, found: C 53.56, H 4.32, S 9.43.

(2*E*)-1-(5-Bromothiophen-2-yl)-3-(4-ethylphenyl)prop-2-en-1-one (**TB6**): Compound **TB6** was isolated as an off-white powder (yield: 95%): mp: 110–112 °C; ^{1}H NMR (400 MHz, $CDCl_3$): δ = 1.27–1.25 (t, 3H, J = 8.0 Hz, CH_3), 2.71–2.69 (q, 2H, J = 8.0 Hz, CH_2), 7.14–7.13 (d, 2H, J = 4.0 Hz, H_4'), 7.25–7.23 (d, 2H, J = 8.0 Hz, H_3 and H_5), 7.29–7.25 (d, 1H, J = 16.0 Hz, CH_α), 7.55–7.53 (d, 2H, J = 8.0 Hz, H_2 and H_6), 7.58–7.57 (d, 2H, J = 4.0 Hz, H_3'), 7.84–7.80 ppm (d, 1H, J = 16.0 Hz, CH_β); ^{13}C NMR (100 MHz, $CDCl_3$): δ = 180.9 (C=O), 147.7 (C_2'), 147.2 (C_β), 144.7 (C_4 and C_3'), 132.4 (C1), 131.3 (C_4'),128.6 (C_2 and C_6), 127.4 (C_3 and C_5), 122.5 (C_5'), 119.5 (Cα), 28.3 (CH_2), 15.6 ppm (CH_3); ESI-MS (*m/z*): calculated 321.23, observed 321.84 $[M]^+$, $[M+2]$; $C_{15}H_{13}BrOS$: C 56.08, H 4.08, S 9.98, found: C 56.12, H 4.32, S 9.92.

(2*E*)-1-(5-Bromothiophen-2-yl)-3-(4-nitrophenyl)prop-2-en-1-one (**TB7**): Compound **TB7** was isolated as a brown powder (yield: 74%): mp: 160–162 °C; ^{1}H NMR (400 MHz, $CDCl_3$): δ = 6.96–6.92 (d, 1H, J = 16.0 Hz, CH_α), 7.14–7.13 (d, 1H, J = 4.0 Hz, H_4'), 7.32–7.31 (d, 1H, J = 4.0 Hz, H_3'), 7.56–7.54 (d, 2H, J = 8.0 Hz, H_2 and H_6), 7.66–7.62 (d, 1H, J = 16.0 Hz, CH_β), 8.23–8.21 ppm (d, 2H, J = 8.0 Hz, H_3 and H_5); ^{13}C NMR (100 MHz, $CDCl_3$): δ = 180.3 (C=O), 147.1 (C_2'), 146.1 (C_4), 145.6 (C_β), 142.4 (C_1), 138.1 (C_3'), 132.0 (C_4'), 127.3 (C_2 and C_6), 122.6 (C_5'), 121.3 (Cα), 120.0 ppm (C_3 and C_5); ESI-MS (*m/z*): calculated 338.17, observed 338.80 $[M]^+$, $[M+2]$; $C_{13}H_8BrNO_3S$: C 46.17, H 2.38; N, 4.14, S 9.48, found: C 46.19, H 2.32; N, 4.24, S, 9.44.

(2*E*)-1-(5-Bromothiophen-2-yl)-3-(4-chlorophenyl)prop-2-en-1-one (**TB8**): Compound **TB8** was isolated as a pale white powder (yield: 98%): mp: 140–142 °C; ^{1}H NMR (400 MHz, $CDCl_3$): δ = 6.96–6.95 (d, 1H, J = 4.8 Hz, H_4'), 7.12–7.11 (d, 1H, J = 4.0 Hz, H_3'), 7.34–7.30 (d, 1H, J = 15.6 Hz, CH_α), 7.57–7.55 (d, 2H, J = 8.0 Hz, H_3 and

H_5), 7.67–7.65 (d, 2H, J=8.0 Hz, H_2 and H_6), 7.80–7.76 ppm (d, 1H, J=16.0 Hz, CH_β); ^{13}C NMR (100 MHz, $CDCl_3$): δ=180.7 (C=O), 145.2 (C_β), 140.1 (C_2'), 139.7 (C_3'), 131.3 (C_4), 130.2 (C_1), 129.1 (C_4'), 128.1 (C_3 and C_5), 127.1 (C_2 and C_6), 122.4 (C_5'), 121.3 ppm (Cα); ESI-MS (*m/z*): calculated 327.62, observed 328.81 $[M]^+$, $[M+2]$, $[M+4]$; $C_{13}H_8ClBrOS$: C 47.66, H 2.46, S 9.79, found: C 47.65, H 2.42, S 9.66.

(2*E*)-3-(4-Bromophenyl)-1-(5-bromothiophen-2-yl)prop-2-en-1-one (**TB9**): Compound **TB9** was isolated as an off-white powder (yield: 55%): mp: 138–140 °C; ^{1}H NMR (400 MHz, $CDCl_3$): δ=6.97–6.93 (d, 1H, J=16.0 Hz, CH_α), 7.14–7.13 (d, 1H, J=4.0 Hz, H_4'), 7.22–7.21 (d, 1H, J=4.0 Hz, H_3'), 7.29–7.27 (d, 2H, J=8.0 Hz, H_2 and H_6), 7.37–7.35 (d, 2H, J=8.0 Hz, H_3 and H_5), 7.57–7.53 ppm (d, 1H, J=16.0 Hz, CH_β); ^{13}C NMR (100 MHz, $CDCl_3$): δ=181.0 (C=O), 147.3 (C_2'), 145.2 (C_β), 138.4 (C_3'), 135.1 (C_1), 132.3 (C_4'), 131.2 (C_3 and C_5), 128.5 (C_2 and C_6), 122.4 (C_4), 121.1 (C_5'), 121.1 ppm (Cα); ESI-MS (*m/z*): calculated 372.07, observed 372.91 $[M]^+$, $[M+2]$, $[M+4]$; $C_{13}H_8BrOS$: C 41.96, H 2.17, S 8.62, found: C 41.66, H 2.22, S 8.83.

(2*E*)-1-(5-Bromothiophen-2-yl)-3-(4-fluorophenyl)prop-2-en-1-one (**TB10**): Compound **TB10** was isolated as an off-white powder (yield: 92%): mp: 128–130 °C; ^{1}H NMR (400 MHz, $CDCl_3$): δ=6.60–6.56 (d, 1H, J=16.0 Hz, CH_α), 6.66–6.64 (d, 2H, J=8.0 Hz, H_2 and H_6),7.14–7.13 (d, 1H, J=4.0 Hz, H_4'), 7.32–7.30 (d, 2H, J=8.0 Hz, H_3 and H_5), 7.52–7.51 (d, 1H, J=4.0 Hz, H_3'), 7.78–7.74 ppm (d, 1H, J=16.0 Hz, CH_β); ^{13}C NMR (100 MHz, $CDCl_3$): δ=180.1 (C=O), 162.3 (C_4), 147.19 (C_2'), 145.4 (C_β), 138.5 (C_3'), 132.4 (C_4'), 130.9 (C_1), 128.6 (C_2 and C_6), 122.5 (C_5'), 121.4 (Cα), 115.6 ppm (C_3 and C_5); ESI-MS (*m/z*): calculated 311.16, observed 311.93 $[M]^+$, $[M+2]$; $C_{13}H_8BrFOS$: C 50.18, H 2.59, S 10.30, found: C 50.38, H 2.44, S 10.18.

(2*E*)-1-(5-Bromothiophen-2-yl)-3-[4-(trifluoromethyl)phenyl]prop-2-en-1-one (**TB11**): Compound **TB11** was isolated as a pale pink powder (yield: 97%): mp: 136–138 °C; ^{1}H NMR (400 MHz, $CDCl_3$): δ=6.66–6.62 (d, 1H, J=15.6 Hz, CH_α), 6.95–6.94 (d, 1H, J=4.0 Hz, H_4'), 7.22–7.20 (d, 2H, J=8.0 Hz, H_2 and H_6), 7.33–7.32 (d, 1H, J=4.0 Hz, H_3'), 7.46–7.44 (d, 2H, J=8.0 Hz, H_3 and H_5), 7.58–7.54 ppm (d, 1H, J=16.0 Hz, CH_β); ^{13}C NMR (100 MHz, $CDCl_3$): δ=180.0 (C=O), 147.4 (C_2'), 145.6 (C_β), 138.3 (C_1), 137.79 (C_3'), 132.7 (C_4'), 130.3 (C_4), 126.7 (C_2 and C_6), 125.1 (C_3 and C_5), 124.5 (CF_3), 122.4 (C_5'), 121.2 ppm (Cα); ESI-MS (*m/z*): calculated 361.17, observed 361.88 $[M]^+$, $[M+2]$; $C_{14}H_8BrF_3OS$: C 46.56, H 2.23, S 8.88, found: C 46.43, H 2.43, S 8.86.

Reagents: Recombinant hMAO-A and hMAO-B (expressed in baculovirus-infected BTI insect cells), R-(−)-deprenyl hydrochloride (selegiline), moclobemide, lazabemide hydrate, resorufin, dimethyl sulfoxide (DMSO), and other chemicals were purchased from Sigma–Aldrich (Munich, Germany). The Amplex Red MAO assay kit (Mybiosource, USA) contained benzylamine, *p*-tyramine, clorgyline, pargyline, and horseradish peroxidase.

Determination of hMAO activity: hMAO activities were determined by a fluorimetric method described and modified previously using *p*-tyramine (0.05–0.50 mM) as a common substrate.[40–42] The study medium contained sodium phosphate buffer (0.1 mL, 0.05 M, pH 7.4), various concentrations of the synthesized compounds or known inhibitors (moclobemide, selegiline and lazabemide), and recombinant hMAO-A or hMAO-B. This mixture was incubated for 15 min at 37 °C in microplates in a dark fluorimeter chamber. The reaction was started by adding Amplex Red reagent (200 μM), horseradish peroxidase (HRP, 1 U mL^{-1}), and *p*-tyramine (0.05–0.50 mM). The production of H_2O_2 catalyzed by MAO isoforms was detected using Amplex Red reagent in the presence of HRP to produce the fluorescent product resorufin. Resorufin was quantified at 37 °C in a multidetection microplate fluorescence reader with excitation at 545 nm and emission at 590 nm over a 15 min period, during which the fluorescence increased linearly. Specific fluorescence emission was calculated after subtraction of the background activity, which was determined from wells containing all components except the hMAO isoforms, which were replaced by a sodium phosphate buffer solution. Under our experimental conditions, this background activity was negligible. Control experiments were carried out by replacing the compound and known inhibitors. The possible capacity of compounds to modify the fluorescence generated in the reaction mixture due to non enzymatic inhibition was determined by adding these compounds to solutions containing only the Amplex Red reagent in a sodium phosphate buffer. The new compounds and reference inhibitors themselves did not react directly with Amplex Red reagent. Newly synthesized compounds did not cause any inhibitory activity of HRP in the test medium.

Kinetics studies: Synthesized compounds were dissolved in DMSO, at a maximum concentration of 1%, and used in a wide compound concentration range of 0.10–1.00 μM. The mode of MAO inhibition was examined using Lineweaver–Burk plotting. The slopes of the Lineweaver–Burk plots were plotted versus the inhibitor concentration, and the K_i values were determined from the x-axis intercept as $-K_i$. Each K_i value is the representative of a single determination in which the correlation coefficient (R^2) of the replot of the slopes versus the inhibitor concentrations was at least 0.98. SI values were calculated as K_i(hMAO-A)/K_i(hMAO-B). The protein concentration was determined according to the Bradford method.[43]

Reversibility of inhibition: Reversibility of MAO inhibition with the compounds was determined by the dialysis method previously described.[44] Dialysis tubing (16×25 mm, Sigma–Aldrich) with a molecular weight cutoff of 12000 Da and a sample capacity of 0.5–10 mL was used. Adequate amounts of the recombinant enzymes (hMAO-A or B, 0.05 mg mL^{-1}) were incubated with a concentration equal to fourfold of the IC_{50} values for the inhibition of hMAO-A and -B, respectively, in potassium phosphate buffer (0.05 M, pH 7.4) containing 5% sucrose and 1% DMSO for 15 min at 37 °C. Another set of enzymes was prepared by pre-incubation of same amount of hMAO-A and -B with the reference inhibitors moclobemide, selegiline, and lazabemide. Enzyme–inhibitor mixtures were subsequently dialyzed at 4 °C in 80 mL of dialysis buffer (100 mM potassium phosphate, pH 7.4) containing 5% sucrose. The dialysis buffer was replaced with fresh buffer at 3 h and 7 h after the start of dialysis. At 24 h after dialysis, residual MAO activities were measured. All reactions were carried out in triplicate, and the residual enzyme catalytic rates were expressed as means ±SEM. For comparison, undialyzed mixtures of the MAOs and the inhibitors were kept at 4 °C over the same time period.

In vitro BBB permeation assay: The ability of newly synthesized compounds that penetrate the BBB was determined using a PAMPA for the BBB, according to a previous method.[35] Briefly, compounds and commercial drugs were dissolved in DMSO at a concentration of 5 mg mL^{-1}. They were diluted with a mixture of phosphate-buffered saline solution and EtOH (PBS/EtOH, 70:30) to give a final concentration of 25 μg mL^{-1}. The filter membrane in the donor microplate was coated with porcine polar brain lipid (PBL) dissolved in dodecane (4 μL, 20 mg mL^{-1}). Diluted solution (200 μL) and PBS/EtOH (70:30, 300 μL) were added to the donor and acceptor wells, respectively. The donor filter plate was carefully placed on the acceptor plate. This sandwich system was stored at 25 °C for 16 h. The donor plate was then carefully removed, and

the concentrations of the compounds and the commercial drugs in the acceptor, donor, and reference wells were measured with a UV plate reader.

Cytotoxic activity: Cell viability was measured by a quantitative colorimetric assay with 3-[4,5 dimethylthiazol-2-yl]-2,5-diphenyltetrazolium bromide (MTT, Sigma–Aldrich). The HepG2 human hepatoma cell line (Invitrogen) was cultured in Dulbecco's modified Eagle's medium (DMEM) supplemented with L-glutamine (2 mM), heat-inactivated fetal bovine serum (FBS, 10%), penicillin (100 U mL^{-1}), and streptomycin (100 μg mL^{-1}). Cells were seeded in supplemented medium and maintained at 37 °C in a humidified atmosphere of 5% CO_2 and 95% air. Exponentially growing HepG2 cells were subcultured in 96-well plates. The cells were treated with the reference MAO inhibitors and novel brominated chalcone compounds (1 μM, 5 μM, and 25 μM) or in 0.1% DMSO as a vehicle control for 24 h. MTT labeling reagent (10 μL), at a final concentration of 5 mg mL^{-1}, was added to each well at the end of the incubation time, and the plate was placed in a humidified incubator at 37 °C with 5% CO_2 and 95% air (*v*/*v*) for 4 h, until purple formazan crystals appeared. Then, the insoluble formazan was dissolved in DMSO (100 μL) by shaking for1 h in the dark. MTT reduction was measured at 590 nm. Control cells treated with 0.1% DMSO were used as 100% viability.[45,46] Significance was determined using Student's t-test. Results were expressed as mean ± SEM. Differences were considered statistically significant at $p < 0.05$.

Molecular docking studies: In the current molecular simulation study, AutoDock 4.2 software was used to establish a ligand-based computer modeling program for the prediction of binding energy of the selected compounds with hMAO isoforms.[47] The docking protocol used X-ray crystal structures of hMAO-A (PDB ID: 2BXR) and hMAO-B (PDB ID: 2BYB) downloaded from the Protein Data Bank (PDB; www.rcsb.org).[48] Protein preparation was carried out using the Protein Preparation Wizard of Maestro 8.5 (Schrödinger, LLC).[49] Ligands were prepared through the PRODRG webserver (davapc1.bioch.dundee.ac.uk/cgi-bin/prodrg).[50] The receptor grids for both enzymes were generated with following parameters: grid box dimension (xyz) of 60×60×60; grid spacing of 0.375 Å, and center of the grid box positioned on the N5 atom of FAD (cofactor). The grid parameter file (.gpf) generated through MGLTools 1.5.6 was then used to generate map types through anautogrid4 execution file. Similarly, for each ligand, a docking parameter file (.dpf) was written using MGLTools 1.5.6 with default parameters except: Number of runs = 50; population size = 300 and number of evaluations = medium. The Lamarckian genetic algorithm was selected for all molecular docking simulations. The .dpf file generated for each ligand was then used for running molecular docking simulations using an AutoDock 4 execution file, which generated docking log files (.dlg) containing results of the simulation. Using the Analyze module in MGLTools 1.5.6, the docking log files were analyzed. The top scoring molecule from the largest cluster was considered for analysis.[51,52]

Acknowledgements

The authors thank the Institute for Intensive Research in Basic Sciences (IIRBS), Mahatma Gandhi University (Kottayam, India) and the Sophisticated Analytical Instrument Facility, Indian Institute of Technology (Chennai, India) for carrying out the spectral analysis.

Keywords: chalcones · cytotoxicity · molecular docking · monoamine oxidases

[1] K. F. Tipton, *Cell Biochem. Funct.* **1986**, *4*, 79–87.
[2] D. Viña, M. J. Matos, G. Ferino, E. Cadoni, R. Laguna, F. Borges, E. Uriarte, L. Santana, *ChemMedChem* **2012**, *7*, 464–470.
[3] T. Rahman, M. Rahmatullah, *Bioorg. Med. Chem. Lett.* **2010**, *20*, 537–540.
[4] J. Shih, K. Chen, M. J. Ridd, *Annu. Rev. Neurosci.* **1999**, *22*, 197–217.
[5] B. Drukarch, F. L. van Muiswinkel, *Biochem. Pharmacol.* **2000**, *59*, 1023–1031.
[6] H. H. Fernandez, J. J. Chen, *Pharmacotherapy* **2007**, *27*, 174S–185S.
[7] A. Petzer, P. Grobler, J. J. Bergh, J. P. Petzer, *J. Pharm. Pharmacol.* **2014**, *66*, 677–687.
[8] C. J. Fowler, A. Wiberg, L. Oreland, J. Marcusson, B. Winblad, *J. Neural Transm.* **1980**, *49*, 1–20.
[9] S. Carradori, J. P. Petzer, *Expert Opin. Ther. Pat.* **2015**, *25*, 91–110.
[10] M. Da Prada, G. Zürcher, I. Wüthrich, W. E. Haefely, *J. Neural Transm. Suppl.* **1988**, *26*, 31–56.
[11] S. Carradori, R. Silvestri, *J. Med. Chem.* **2015**, *58*, 6717–6732.
[12] Z. A. Nowakowska, *Eur. J. Med. Chem.* **2007**, *42*, 125–137.
[13] N. K. Sahu, S. S. Balbhadra, J. Choudhary, D. V. Kohli, *Curr. Med. Chem.* **2012**, *19*, 209–225.
[14] B. Mathew, J. Suresh, S. Anbazghagan, J. Paulraj, G. K. Krishnan, *Biomed. Prev. Nutr.* **2014**, *4*, 451–458.
[15] P. Singh, A. Anand, V. Kumar, *Eur. J. Med. Chem.* **2014**, *85*, 758–777.
[16] D. K. Mahapatra, V. Asati, S. K. Bharti, *Eur. J. Med. Chem.* **2015**, *92*, 839–865.
[17] D. Secci, S. Carradori, A. Bolasco, B. Bizzarri, M. D'Ascenzio, E. Maccioni, *Curr. Top. Med. Chem.* **2012**, *12*, 2240–2257.
[18] B. Mathew, J. Suresh, S. Anbazhagan, G. E. Mathew, *Cent. Nerv. Syst. Agents Med. Chem.* **2013**, *13*, 195–206.
[19] S. Tanaka, Y. Kuwai, M. Tabata, *Planta Med.* **1987**, *53*, 5–8.
[20] F. Chimenti, R. Fioravanti, A. Bolasco, P. Chimenti, D. Secci, F. Rossi, M. Yáñez, F. Orallo, F. S. Alcaro, *J. Med. Chem.* **2009**, *52*, 2818–2824.
[21] S. J. Robinson, J. P. Petzer, A. Petzer, J. J. Bergh, A. C. U. Lourens, *Bioorg. Med. Chem. Lett.* **2013**, *23*, 4985–4989.
[22] G. Jo, S. Ahn, B. G. Kim, H. R. Park, Y. H. Kim, H. A. Choo, D. Koh, Y. Chong, J. H. Ahn, Y. Lim, *Bioorg. Med. Chem.* **2013**, *21*, 7890–7897.
[23] N. Morales-Camilo, C. O. Salas, C. Sanhueza, C. Espinosa-Bustos, M. Reyes-Parada, F. Gonzalez-Salas, C. Sanhauez, C. Espinosa-Bustos, S. Sepulveda-Boza, M. Reyes-Parada, F. Gonzalez-Nilo, M. Caroli-Rezende, A. Fierro, *Chem. Biol. Drug Des.* **2015**, *85*, 685–695.
[24] J. W. Choi, B. K. Jang, N. Cho, J. H. Park, S. K. Yeon, E. J. Ju, Y. S. Lee, G. Han, A. M. Pae, D. J. Kim, K. D. Park, *Bioorg. Med. Chem.* **2015**, *23*, 6486–6496.
[25] S. Zaib, S. U. F. Rizvi, S. Aslam, M. Ahmad, S. M. A. Abid, M. al-Rashida, J. Iqbal, *Med. Chem.* **2015**, *11*, 580–589.
[26] S. Zaib, S. U. F. Rizvi, S. Aslam, M. Ahmad, M. al-Rashida, J. Iqbal, *Med. Chem.* **2015**, *11*, 497–505.
[27] C. Minders, J. P. Petzer, A. Petzer, A. C. U. Lourens, *Bioorg. Med. Chem. Lett.* **2015**, *25*, 5270–5276.
[28] B. Mathew, G. E. Mathew, G. Uçar, I. Baysal, J. Suresh, J. K. Vilapurathu, A. Prakasan, J. K. Suresh, A. Thomas, *Bioorg. Chem.* **2015**, *62*, 22–29.
[29] B. Mathew, G. Uçar, S. Y. Ciftci, I. Baysal, J. Suresh, G. E. Mathew, J. K. Vilapurathu, N. A. Moosa, N. Pullarottil, L. Viswam, A. Haridas, F. Fathima, *Lett. Org. Chem.* **2015**, *12*, 605–613.
[30] M. B. H. Youdim, Y. S. Bakhle, *Br. J. Pharmacol.* **2006**, *147*, S287–S296.
[31] R. Ramsay, *Curr. Top. Med. Chem.* **2012**, *12*, 2189–2209.
[32] C. Binda, E. M. Milczek, D. Bonivento, J. Wang, A. Mattevi, D. E. Edmondson, *Curr. Top. Med. Chem.* **2011**, *11*, 2788–2796.
[33] W. A. Banks, *BMC Neurol.* **2009**, *9*, S3.
[34] M. P. Schaddelee, H. L. Voorwinden, D. Groenendaal, A. Hersey, A. P. Ijzerman, M. Danhof, A. G. De Boera, *Eur. J. Pharm. Sci.* **2003**, *20*, 347–356.
[35] L. Di, E. H. Kerns, K. Fan, O. J. McConnell, G. T. Carter, *Eur. J. Med. Chem.* **2003**, *38*, 223–232.
[36] C. Binda, M. Li, F. Hubalek, N. Restelli, D. E. Edmondson, *Proc. Natl. Acad. Sci. USA* **2003**, *100*, 9750–9755.

[37] L. Legoabe, J. Kruger, A. Petzer, J. J. Bergh, J. P. Petzer, *Eur. J. Med. Chem.* **2011**, *46*, 5162 – 5174.
[38] R. K. Tripathi, S. Krishnamurty, S. R. Ayyannan, *ChemMedChem* **2016**, *11*, 119 – 132.
[39] F. Manna, F. Chimenti, F. A. Bolasco, D. Secci, B. Bizzarri, O. Befani, P. Turini, B. Mondovi, S. Alcaroc, A. Tafi, *Bioorg. Med. Chem. Lett.* **2002**, *12*, 3629 – 3633.
[40] M. C. Anderson, F. Hasan, J. M. McCrodden, K. F. Tipton, *Neurochem. Res.* **1993**, *18*, 1145 – 1149.
[41] M. Yáñez, N. Fraiz, E. Cano, F. Orallo, *Biochem. Biophys. Res. Commun.* **2006**, *344*, 688 – 695.
[42] F. Chimenti, E. Maccioni, D. Secci, A. Bolasco, P. Chimenti, A. Granese, S. Carradori, S. Alcaro, F. Ortuso, M. Yáñez, *J. Med. Chem.* **2008**, *51*, 4874 – 4880.
[43] M. M. Bradford, *Anal. Biochem.* **1976**, *72*, 248 – 254.
[44] A. Petzer, A, Pienaar, J. P. Petzer, *Life Sci.* **2013**, *93*, 283 – 287.
[45] M. B. Hansen, S. E. Nielsen, K. Berg, *J. Immunol. Methods* **1989**, *119*, 203 – 210.
[46] C. F. Wu, R. Bertorelli, M. Sacconi, G. Pepeu, S. Consolo, *Neurobiol. Aging* **1988**, *9*, 357 – 361.
[47] G. M. Morris, R. Huey, W. Lindstrom, M. F. Sanner, R. K. Belew, D. S. Goodsell, A. J. Olson, *J. Comput. Chem.* **2009**, *30*, 2785 – 2791.
[48] L. De Colibus, M. Li, C. Binda, A. Lustig, D. E. Edmondson, A. Mattevi, *Proc. Natl. Acad. Sci. USA* **2005**, *102*, 12684 – 12689.
[49] B. Vishnu Nayak, S. Ciftci-Yabanoglu, S. S. Jadav, M. Jagrat, B. N. Sinha, G. Ucar, V. Jayaprakash, *Eur. J. Med. Chem.* **2013**, *69*, 762 – 767.
[50] A. W. Schüttelkopf, D. M. van Aalten, *Acta Crystallogr. Sect. D* **2004**, *60*, 1355 – 1363.
[51] B. V. Nayak, S. Ciftci-Yabanoglu, S. Bhakat, A. K. Timiri, B. N. Sinha, G. Ucar, M. E. S. Soliman, V. Jayaprakash, *Bioorg. Chem.* **2015**, *58*, 72 – 80.
[52] V. N. Badavath, I. Baysal, G. Ucar, S. K. Mondal, B. N. Sinha, V. Jayapraksh, *Arch. Pharm. Chem. Sci. Ed.* **2016**, *349*, 9 – 19

Received: March 1, 2016
Revised: March 30, 2016
Published online on May 9, 2016